Energy Storage Capacity Optimization of Non-Grid-Connected Wind-Hydrogen Systems: From the Perspective of Hydrogen Production Features

Xinyu Zhang[1], Hua Li[2*], Jikang Wang[1]

[1] School of Electrical, Inner Mongolia University of Technology, 010080 Hohhot, China
[2] School of Energy and Power Engineering, Inner Mongolia University of Technology, 010051 Hohhot, China

* Correspondence: Hua Li (lihua1028@imut.edu.cn)

Abstract: This paper intends to improve the hydrogen production efficiency of the electrolysis cells, fully utilize wind energy, and ensure the reliability of power supply. For this purpose, the authors put forward a capacity optimization configuration for non-grid-connected wind-hydrogen hybrid energy storage system, in view of the features of hydrogen production efficiency. The working interval of the electrolytic cell was optimized by analyzing the said features. Considering the features of battery charge/discharge, equipment capacity and power, the authors formulated the energy management strategy applicable to six working conditions, established the quantitative multi-objective function of system cost and reliability, and solved the optimization model by the fast non-dominant sorting genetic algorithm (NSGA)-II. In this way, the optimal combination of energy storage capacity was determined. Next, the wind velocity data of a pastoral area in Inner Mongolia was measured, and analyzed in details. The analysis results show that the electrolytic cell always operates in the optimal working area, and the optimized wind-hydrogen system is economic and reliable in power supply. The research provides a reference for practical engineering applications.

Keywords: Hydrogen production features; Wind-hydrogen system; Electrolytic cell; Hybrid energy storage; Capacity optimization; Fast non-dominant sorting genetic algorithm (NSGA)-II

1. Introduction

Many countries are actively pursuing carbon neutrality and carbon peaking by promoting the development of hydrogen energy, which stimulates the growth of renewable energy generation. To achieve the two objectives, it is crucial to couple hydrogen energy with renewable energy, optimize the synergy of multiple energy sources for electricity and heating, promote the advances of distributed energy, make better use of terminal energy, and realize the coupling development between renewable energies (e.g., hydrogen energy and wind power).

Off-grid wind power mode refers to the concept of connecting to the grid without a grid connection, eliminating the impact of wind power on the grid and realizing the efficient use of wind power [1]. The output terminal of wind power is no longer a single grid but rather an industry or other field that can adapt to the features of wind power. As a new technical solution to the issue of wind power consumption, the hybrid energy storage system formed by hydrogen storage and storage batteries under off-grid conditions can efficiently smooth out wind power fluctuations and improve the dispatchability of wind power. The related energy management strategy and capacity optimization configuration have gradually become a research hotspot, attracting the attention from most experts and scholars.

The research on the capacity optimization configuration and energy management strategy of wind-hydrogen hybrid energy storage systems has made some significant advancements thanks to the unceasing exploration by professionals and academics both domestically and internationally. In order to meet the national grid-connected standard and effectively smooth out wind power fluctuation, Nie et al. [2] proposed a low-pass filter-based alkaline electrolysis cell-battery hybrid energy storage configuration method and developed a hydrogen-super hybrid

energy storage system control strategy based on the state of charge (SOC) of the battery. These methods do not consider the effects of load shortage rate on capacitive loads. To optimize the energy storage capacity that balances economy and reliability, Liang et al. built a grid-connected wind-hydrogen hybrid energy storage system with energy-based energy storage containing hydrogen and power-based energy storage with batteries [3, 4]. They also developed an energy management strategy, but failed to model the curtailment of wind power. Cai et al. [5] proposed an enhanced chemical reaction algorithm based on the complementing benefits of particle swarm and chemical reaction optimization methods for grid-connected wind, hydrogen, and combustion systems.

Based on system installation costs, load default rates, and output power fluctuations, Ma et al. [6] presented the capacity allocation for off-grid wind-hydrogen complementary systems, which effectively ensures the economy and reliability of the power supply but does not take into account the effect of operating costs on system economics. Zhang et al. [7] put forward an effective optimization algorithm for optimization and long-term capacity planning of the off-grid hybrid renewable energy system, which is made up of hydrogen storage, fuel cells, and wind power. They also suggested three improved global dynamic harmony search methods and analyzed the effects of various maximum iteration times and reliability levels on system capacity configuration. Zhang et al. [8] derived the most economically advantageous configuration for hydrogen and renewable energy scenery systems by integrating hybrid search optimization algorithms with weather forecast data. Basu et al. [9] examined the economic costs of three systems—wind-hydrogen, solar-hydrogen, and wind-solar-hydrogen—using the HOMER program, concluding that the wind-solar-hydrogen system is the most cost-effective system. Zhang et al. studied only the cost without taking the security of the power supply into account [8, 9]. This leaves out the assessment of hydrogen generation efficiency.

The system's safety and dependability should not be overlooked, however, as production halts and downtime brought on by a power supply that is less reliable can substantially cost consumers money and retard social and economic advancement. A problem that needs to be solved right now is how to create a fair structure for the wind-hydrogen storage system and, through capacity optimization and energy management strategies, achieve good system economy, high hydrogen production efficiency, and at the same time guarantee safe and dependable power supply.

In view of the above problems, this paper formulates an energy management strategy by analyzing the hydrogen production efficiency of the electrolytic cell and the charging and discharging features of the battery, and proposes an optimization method for hybrid energy storage capacity of the wind hydrogen system, in view of the hydrogen production efficiency features of the electrolytic cell. The total cost of the system, the power shortage rate of the load and the power fluctuation rate were taken as the objective functions. On this basis, the fast non-dominant sorting genetic algorithm (NSGA)-II was employed to solve the problem, and obtains an economic and reliable capacity combination, which enables the electrolyzer to operate within the optimal operating range. Simulation results show that the proposed optimization method and energy management strategy are both correct and effective.

2. Wind-Hydrogen System

As shown in Figure 1, the off-grid wind-hydrogen hybrid energy storage system consists of a wind turbine, a battery, a hydrogen storage tank, a hydrogen production system (electrolyzer), a fuel cell and a converter. Specifically, the electrolyzer dissipates excess wind power, the hydrogen fuel cell supplies energy to the outside when the wind power output is insufficient, and the battery serves as a flexible storage unit to assist the hydrogen storage for dissipating wind power and compensating for the load demand.
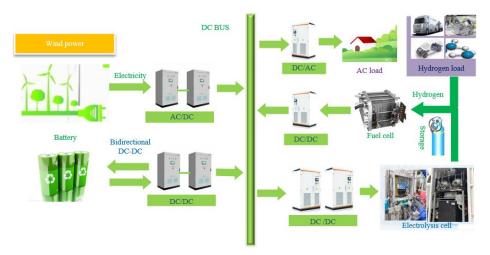

Figure 1. Structure of the wind-hydrogen system

2.1 Mathematical Models

2.1.1 Wind turbine

Ignoring the time lag effect and wake effect of the wind farm, the output power of the wind turbine can be expressed as [5]:

$$P_{wt} = \begin{cases} 0 & V < V_{in}, V > V_{out} \\ P_N \dfrac{V^3 - V_{in}^3}{V_N^3 - V_{in}^3} & V_{in} \leq V < V_N \\ P_N & V_N \leq V < V_{out} \end{cases} \tag{1}$$

where, P_N is the rated output of the wind turbine; V_{in} is the cut-in wind velocity; V_{out} is the cut-out wind velocity; V is the actual wind velocity; V_N is the rated wind velocity.

2.1.2 Hydrogen energy storage system

This paper develops a hydrogen storage system with polymer electrolyte membrane (PEM) electrolysis cells for hydrogen production, after selecting storage tank for gaseous pressurized hydrogen and a PEM fuel cell. Compared with the traditional alkaline electrolysis cells, the PEM electrolysis cells boast a wide load range, flexible operation and fast response. The storage of high pressure gaseous compressed hydrogen is cheaper and more efficient in conversion than the conventional storage technologies [10]. With a power density of 0.35-1.0W/cm^2, PEM fuel cells can deliver greater power values per unit volume of hydrogen consumed. Hence, PEM electrolysis cells are the most suitable power generation device for hydrogen production and storage systems.

The electrolysis cells use excess wind power to produce hydrogen. The amount Q_{el} of hydrogen produced by the electrolysis cells (Nm^3) can be calculated by:

$$Q_{el} = P_{el} \times \eta_{el} \times \rho \tag{2}$$

where, P_{el} is the input power of the electrolysis cells; η_{el} is the efficiency of the electrolysis cells; ρ is the amount of hydrogen produced per 1 kWh electrical energy (0.22 Nm^3/kWh).

The output power of the fuel cells can be calculated by:

$$P_{fc} = \frac{Q_{fc}}{\mu} \bullet \eta_{fc} \tag{3}$$

where, Q_{fc} is the amount of hydrogen input to the fuel cell, Nm^3; η_{fc} is the fuel cell efficiency; μ is the amount of hydrogen required to produce $1kWh$ electrical energy (0.6434 Nm^3/kWh).

The hydrogen storage capacity of the storage tank can be calculated by:

$$Q_{ht}(t) = Q_{ht}(t-1) + Q_{el}(t)\Delta t - \frac{P_{fc}(t) \bullet \mu \bullet \Delta t}{\eta_{fc} \bullet \eta_{ht}} \tag{4}$$

where, $Q_{ht}(t)$ is the amount of hydrogen in the storage tank at time t; $Q_{el}(t)$ is the amount of hydrogen produced by the electrolysis cells at time t; $P_{fc}(t)$ is the fuel cell output at time t; η_{ht} is the storage efficiency of the storage tank; Δt is the sampling interval.

The SOC of the hydrogen energy storage can be expressed as:

$$SOC_{ht}(t) = Q_{ht}(t) / Q_{htmax} \tag{5}$$

where, Q_{htmax} is the maximum storage capacity of the hydrogen tank.

2.1.3 Battery model

As an auxiliary energy storage for the wind-hydrogen system, the battery not only helps the hydrogen storage stabilize wind power fluctuations and address the issue of wind curtailment, but also provides the electrolyzer with power when the remaining wind power is below the minimum input power that the electrolyzer can accept, allowing it to function at its best.

The SOC of a battery can be expressed as:

$$SOC(t) = E_{sc}(t) / E_{scmax} \tag{6}$$

where, $E_{sc}(t)$ and E_{scmax} are the remaining charge and the maximum charge of the battery at the current moment, respectively. As charging and discharging proceeds, the SOC of the battery rises or falls according to the following relationship:

$$\begin{cases} SOC(t)_1 = (1-\Delta) \cdot SOC(t-1)_1 + \dfrac{P_{ch} \cdot \Delta_t \cdot \eta_{ch}}{E_{sc}} \\ SOC(t)_2 = (1-\Delta) \cdot SOC(t-1)_2 + \dfrac{P_{dis} \cdot \Delta_t \cdot \eta_{dis}}{E_{sc}} \end{cases} \tag{7}$$

where, Δ is the self-discharge rate of the battery, 0.01; $SOC(t)_1$ and $SOC(t)_2$ are the SOC values of the battery during charging and discharging, respectively; P_{ch} and P_{dis} are the charging and discharging powers, respectively; η_{ch} and η_{dis} are the charging and discharging efficiencies of the battery, respectively; E_{sc} is the rated capacity of the battery; Δ_t is the charging or discharging interval of the battery.

2.2 Efficiency Features of Electrolysis Cell

PEM electrolysis cells are well adapted to the fluctuations of wind power and can operate in the load range of 5 to 120%, whereas wind power resources are highly volatile and stochastic, leading to unstable wind power production [11]. The electrolytic cell's unit current density is correlated with the hydrogen production efficiency. The higher the unit current density when electrolyzing water, the better the hydrogen production efficiency. The electrolysis cell's hydrogen production efficiency features need to be examined in order to establish its ideal operating interval.

The water electrolysis voltage of a PEM electrolysis cell depends on the unit current density during the electrolysis of water at a specific temperature and pressure [12]:

$$U_{el}(T,P,j) = U_{rev}(T,P) + U_{ohm}(j) + U_{h2}(T,P,j) + U_{o2}(T,P,j) \tag{8}$$

$$U_{rev}(T,P) = 1.5184 - 1.5421 \times 10^{-3} T + 9.523 \times 10^{-5} T \log_e T + 9.84 \times 10^{-8} T^2$$

$$\begin{aligned} U_{ohm}(j) &= j \sum_{i=1}^{n} R_i \\ U_{h2}(T,P,j) &= \frac{RT}{\alpha_c n_c F} \ln\left(\frac{j}{j_{co}}\right) \\ U_{o2}(T,P,j) &= \frac{RT}{\alpha_a n_a F} \ln\left(\frac{j}{j_{ao}}\right) \end{aligned} \tag{9}$$

where, j is the unit current density of the electrolyzer; $U_{rev}(T,P)$ is the reversible voltage required by the electorlyer to electrolyze water; $U_{ohm}(j)$ is the pressure drop caused by the surface resistance of the electrolyzer; $U_{h2}(T,P,J)$ and $U_{o2}(T,P,J)$ are the hydrogen and oxygen superpotentials generated during water electrolysis, respectively; F is the Faraday constant; R_i is the surface resistance of the i-th cell component; R is the ideal gas constant; α_c and α_a are the charge transfer coefficients of the cathode and anode, respectively; n_c and n_a are the electron transfer numbers of the cathode and anode, respectively; j_{co} and j_{ao} are the exchange current densities of the cathode and anode, respectively.

The voltage efficiency of an electrolysis bath is the ratio of the theoretical decomposition voltage to the actual decomposition voltage of water. The water electrolysis is heated up by electrical energy. Thus, the theoretical decomposition voltage is replaced by the thermal neutral voltage. Thus, the voltage efficiency can be expressed as:

$$\eta_v = (U_{tn} / U_{el}) \times 100\% \tag{10}$$

The relationship between power and the amount of hydrogen generated is not adequately depicted by an electrolyzer's voltage efficiency, which simply measures how effectively electrical energy is utilized by the

electrolyzer [13]. Both voltage efficiency and current efficiency are related to the efficiency of hydrogen production in an electrolyzer. At various pressures and temperatures, the electrolytic cell's current efficiency varies. The current efficiency (Faraday efficiency) of the electrolyer, under constant temperature and pressure, can be expressed as:

$$\eta_i = 96.5e^{0.09/I_{el} - 75.5/I_{el}^2} \tag{11}$$

where, I_{el} is the stack current of the electrolyzer, $I_{el} = A \cdot j$, with A being the cross-sectional area of the electrolyzer.

The hydrogen production efficiency of the electrolysis tank can be expressed as:

$$\eta_{el} = \eta_v \cdot \eta_i \tag{12}$$

The parameters of electrolysis cell are listed in Table 1 [14]:

Table 1. Parameters of electrolyzer

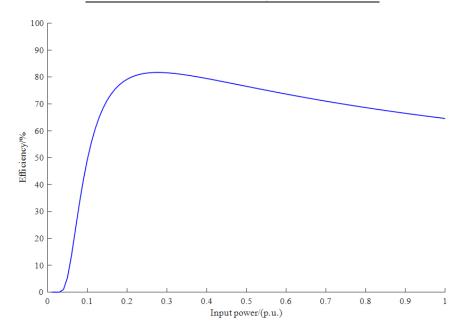| Parameters	Values
Operating temperature T/K	353.15
Pressure P/Pa	1.01×10^5
Thermally neutral voltage U_{tn}/V	1.48
Unit current density $j/A \cdot cm^{-2}$	0~2
Surface resistance $R_i/m\Omega$	26.8
Cross-sectional area A/cm^2	50
Faraday constant $F/C \cdot mol^{-1}$	96485.3
Ideal gas constant $R/J \cdot mol^{-1} \cdot K^{-1}$	8.31446
Cathode charge transfer coefficient α_c	0.71
Anode charge transfer coefficient α_a	0.29
Cathode exchange current density $j_{co}/mA \cdot cm^{-2}$	24.6
Anode exchange current density $j_{ao}/mA \cdot cm^{-2}$	24.1
Electron transfer numbers n_c, n_a	2

Figure 2. Efficiency feature curve of hydrogen production

The relationship between the input power (the nominal value) and the hydrogen generation efficiency in an electrolysis cell was established by Eqns. (8)-(12). The hydrogen production efficiency in the electrolysis cell reached 81.69%, as shown in Figure 2, and it was favorably associated with the initial input power, peaking at about 0.3. When the input power reached its rated power, the electrolysis cell's efficiency was about 65%. As the input power rose further, the efficiency of the electrolysis cell gradually declined. When running at lower loads compared to the rated load, the water electrolysis system's electrolysis cell section can drastically cut energy usage

and boost hydrogen production efficiency. The efficiency of the electrolysis cell is low and the amount of hydrogen produced is limited when the electrolysis cell is run at a low load factor of 0-20%. The ideal working range of the electrolysis cell is chosen at 30 to 100% of the rated power, taking into account the coupling relationship between hydrogen production efficiency and input power.

2.3 Energy Management Strategy

The energy management approach depicted in Figure 3 was devised, in the light of the battery's charging and discharging capabilities and the working interval of the hydrogen generation process. Figure 3 describes the electrolytic cell, battery, and fuel cell processes under the six operating conditions of the system mathematically.
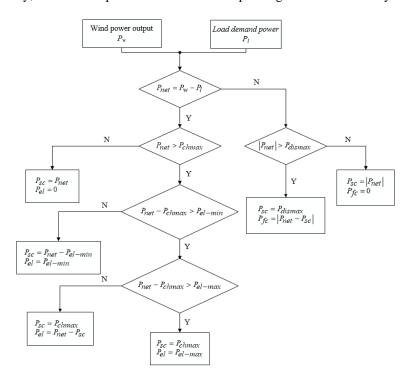

Figure 3. Energy management strategy

For a given sampling interval, the net output power of the system can be described by:

$$P_{net} = P_w - P_l \tag{13}$$

The lower and upper limits of the optimum operating interval of the electrolytic cell are denoted by $P_{el\text{-}min}$ and $P_{el\text{-}min}$, respectively; the maximum allowable charge and discharge power of the battery are denoted by P_{chmax} and P_{chmin}, respectively.

2.3.1 Absorption of curtailed wind
The electrolysis cell produces hydrogen, or the battery charges and the fuel cell is out of service, when the net power is more than 0 (load demand is less than the amount of wind energy produced).
Mode 1: The system functions in mode 1 when the net power is lower than the maximum permitted battery charge power. In this case, the battery is charged normally and both the electrolytic cell and fuel cell are out of service. Then, the charging power of the batteries can be calculated by:

$$P_{net} \leq P_{chmax} \tag{14}$$

$$P_{sc} = P_{net} \tag{15}$$

Mode 2: When the system satisfies Eq. (16), the input power of the electrolytic cell and the charging power of the battery satisfy Eq. (17):

$$P_{net} - P_{chmax} < P_{el-min} \tag{16}$$

$$\begin{cases} P_{el} = P_{el-min} \\ P_{sc} = P_{net} - P_{el-min} \end{cases} \tag{17}$$

At this point, the electrolyzer is producing hydrogen at the minimum allowable input power. The charging and discharging of the battery depend on the difference between the net power of the system and the minimum allowable input power of the electrolyzer during this sampling interval. If $\boldsymbol{P_{net} - P_{el-min}}$, the battery is charged; If $P_{net} - P_{el-min}$, the battery is discharged to assist the electrolyzer in producing hydrogen at the minimum allowable input power.

Mode 3: When the system satisfies Eq. (18), the input power of the electrolytic cell and the charging power of the battery satisfy Eq. (19):

$$P_{el-min} \le P_{net} - P_{chmax} \le P_{el-max} \tag{18}$$

$$\begin{cases} P_{el} = P_{net} - P_{chmax} \\ P_{sc} = P_{chmax} \end{cases} \tag{19}$$

In this case, the electrolytic cell operates within the optimal interval, and the battery is charged at the maximum allowable charging power.

Mode 4: When the system satisfies Eq. (20), the input power of the electrolytic cell, the charging power of the battery and the curtailed wind power of the wind farm satisfy Eq. (21):

$$P_{net} - P_{chmax} > P_{el-max} \tag{20}$$

$$\begin{cases} P_{el} = P_{el-max} \\ P_{sc} = P_{chmax} \\ P_{qf} = P_{net} - P_{el} - P_{sc} \end{cases} \tag{21}$$

In this case, the electrolyzer operates at the rated input power, the battery is charged at the maximum allowable charging power, and the excess wind power is curtailed.

2.3.2 Energy storage systems during discharge

When the net power is less than 0 (wind power output is less than the load demand), the electrolysis cell is shut down and the battery and fuel cell are discharged.

Mode 5: When the system satisfies Eq. (22), the fuel cell is out of service and the battery is discharged normally. The discharge power can be expressed by Eq. (23):

$$|P_{net}| \le P_{dismax} \tag{22}$$

$$P_{sc} = |P_{net}| \tag{23}$$

Model 6: When the system satisfies Eq. (24), the battery, fuel cell discharge power and system deficit power can be expressed by Eq. (25):

$$|P_{net}| > P_{dismax} \tag{24}$$

$$\begin{cases} P_{sc} = P_{dismax} \\ P_{fc} = |P_{net}| - P_{sc} \\ P_{qe} = |P_{net}| - P_{sc} - P_{fc} \end{cases} \tag{25}$$

In this case, the battery discharges first at the maximum allowable discharge power and the fuel cell discharges subsequently. The power shortage will ensue, for the battery and fuel cell are limited in capacity, and there is an imbalance between supply and demand.

3. Capacity Optimization Model

3.1 Objective Function

Consdiering the need to meet the demand for wind power disposal and smooth power supply, the capacity of hydrogen storage and storage batteries in the system should be configured to maximize the economy of the system, and to ensure the reliability of the power supply. In this paper, the capacity optimization model is solved through optimization, followed by decision-making. In this case, the total cost and reliability indicator have the same weight, and the capacity of each part of the energy storage device is determined by the principle of compromise.

3.1.1 Economic cost analysis
The total cost of hybrid energy storage can be expressed as:

$$C_{Total} = C_{INV} + C_{O\&M} + C_{REP} + C_{QF} \tag{26}$$

where, C_{INV} is the initial investment cost of the system; $C_{O\&M}$ is the operation and maintenance cost of the system; C_{REP} is the replacement cost of the system equipment; C_{QF} is the cost of system wind curtailment. The initial investment cost of the system can be expressed as:

$$C_{INV} = C_{EL} \times K_{EL} + C_{SC} \times K_{SC} + C_{HT} \times K_{HT} + C_{FC} \times K_{FC} \tag{27}$$

where, C_{EL}, C_{SC}, C_{HT}, and C_{FC} are the capacities of the electrolyzer, battery, hydrogen storage tank and fuel cell respectively, and also the decision variables of capacity optimization; K_{EL}, K_{SC}, K_{HT}, and K_{FC} are the unit prices of the respective equipment in ¥/kW or ¥/kWh. The operation and maintenance cost of the system can be expressed as:

$$C_{O\&M} = \partial \times C_{INV} \tag{28}$$

where, ∂ is the proportionality factor, which represents the share of the system operation and maintenance costs in the total initial investment cost.

$$
\begin{aligned}
C_{REP} = &C_{SC} \times K_{SC} \times \sum_{a=1}^{N/L_{sc}} \frac{1}{(1+i)^{a \times L_{sc}}} + C_{EL} \times K_{EL} \times \sum_{b=1}^{N/L_{el}} \frac{1}{(1+i)^{b \times L_{el}}} \\
&+ C_{HT} \times K_{HT} \times \sum_{c=1}^{N/L_{ht}} \frac{1}{(1+i)^{c \times L_{ht}}} \\
&+ C_{FC} \times K_{FC} \times \sum_{d=1}^{N/L_{fc}} \frac{1}{(1+i)^{d \times L_{fc}}}
\end{aligned} \tag{29}
$$

where, L_{sc}, L_{el}, L_{ht}, and L_{fc} are the service life of the battery, electrolytic tank, hydrogen storage tank and fuel cell, respectively; i is the annual interest rate, $i=0.04$; N is the operating cycle of the wind-hydrogen system, $N=20$.

There are two main causes of the wind curtailment phenomenon in the wind-hydrogen system: first, the energy storage system has a limitation on the amount of wind power that can be consumed, or the wind curtailment is produced when the system is in mode 4; second, the wind curtailment happens when the system's storage capacity reaches its maximum and the remaining wind turbine power is no longer fed into the electrolyzer unit. The cost of the wind curtailment is calculated using the power that was reduced and added to an objective function of the total cost. The greater the power reduction, the higher the penalty cost.

$$C_{QF} = \rho_1 \times \sum_{t=1}^{T} P_{net}(t) - P_{el}(t) - P_{sc}(t) + P_{h2}(t) \Big|_{Q_{el}(t)\Delta t > Q_{ht\,max} - Q_{ht}(t)} \tag{30}$$

where, ρ_1 is the unit cost of wind curtailment, 5.8 ¥/kWh [15-20]; $P_{net}(t)$, $P_{el}(t)$ and $P_{sc}(t)$ are the net power at the t-th sampling point, the electrolyzer input power and the battery charging power. when the system is operating in mode 4, respectively; $P_{h2}(t)$ is the curtailed wind power generated under the hydrogen production constraint of the electrolyzer; T is the number of sampling points.

3.1.2 Reliability analysis

Power fluctuation rate and power deficit rate are selected to measure the reliability of the power supply.

The power volatility reflects the smoothness of the system output power and is expressed as the percentage change in power at each sampling moment of that system's output power:

$$P_{total}(t) = P_W(t) + P_{sc}(t) - P_{el}(t) + P_{fc}(t)$$

$$f_{FPP} = \frac{\sum\limits_{t=1}^{T-1} \left[P_{total}(t+1) - P_{total}(t) \right]}{\sum\limits_{t=1}^{T} P_{total}(t)} \tag{31}$$

where, $P_w(t)$ is the output power of the wind turbine at the t-th sampling point; $P_{sc}(t)$ is the output power of the battery; $P_{el}(t)$ is the input power of the electrolyzer; $P_{fc}(t)$ is the output power of the fuel cell; $P_{total}(t)$ is the output power of the system at the t-th sampling point; $P_{total}(t+1)$ is the output power of the system at the $(t+1)$ th sampling point.

The load shortage rate reflects the probability of a load failing to meet its power demand and is expressed as the ratio of the amount of unmet load demand in each sampling period to the demand of the load in that period.

$$f_{LPSP} = \frac{\sum\limits_{t=1}^{T} P_{qe}(t)}{\sum\limits_{t=1}^{T} P_l(t)} \tag{32}$$

where, $P_l(t)$ is the demand power of the load at the t-th sampling point; $P_{qe}(t)$ is the shortfall power of the load at the t-th sampling point.

According to the entropy weight method, the weight indicators of power fluctuation rate and load shortage rate are 0.46 and 0.54 respectively. Considering the economic cost, the objective functions of the system are:

$$\begin{cases} f_1 = C_{INV} + C_{O\&M} + C_{REP} + C_{QF} \\ f_2 = 0.46 f_{FPP} + 0.54 f_{LPSP} \end{cases} \tag{33}$$

3.2 Binding Conditions

1) Equipment capacity constraints

$$\begin{aligned} & 0 < C_{EL} < C_{EL}^{max} \\ & 0 < C_{SC} < C_{SC}^{max} \\ & 0 < C_{HT} < C_{HT}^{max} \\ & 0 < C_{FC} < C_{FC}^{max} \\ & C_{EL}, C_{SC}, C_{HT}, C_{FC} \in R^+ \end{aligned} \tag{34}$$

where, *Cmax EL*, *Cmax SC, Cmax HT,* and *Cmax FC* are the upper capacity limits of the electrolyzer, battery, hydrogen storage tank and fuel cell respectively.

2) Battery charging and discharging constraints

$$
\begin{cases}
SOC_{min} < SOC(t) < SOC_{max} \\[2mm]
P_{chmax} = \min\left\{ P_{cmax}^{sc}, P_{chmax}^{sc}(t) \right\} \\[2mm]
P_{dismax} = \min\left\{ P_{dmax}^{sc}, P_{dismax}^{sc}(t) \right\} \\[2mm]
P_{chmax}^{sc}(t) = \dfrac{E_{sc}\left[SOC(t) - (1-\Delta)SOC(t-1) \right]}{\eta_{ch} \bullet \Delta_t} \\[4mm]
P_{dismax}^{sc}(t) = \dfrac{E_{sc} \bullet \eta_{dis} \bullet \left[SOC(t) - (1-\Delta)SOC(t-1) \right]}{\Delta_t}
\end{cases}
\tag{35}
$$

where, SOC_{min}, and SOC_{max} are the upper and lower limits of the charge state of the battery; P_{chmax}, and P_{chmax} are the maximum allowable charge and discharge power of the battery at sampling time t; $Psc\ cmax$, and $Psc\ dmax$ are the maximum continuous charge and discharge power of the battery, determined by its charge and discharge features; $Psc\ chmax(t)$, and $Psc\ dismax(t)$ are the maximum allowable charge and discharge power of the battery at sampling time t, determined by its rated capacity and charge state.

3) Power constraint on electrolyzer operation

$$
P_{el-min} < P_{el} < P_{el-max}
\tag{36}
$$

where, P_{el-min}, and P_{el-max} are the upper and lower limit of the optimum operating power of the electrolyzer, with the lower limit being 30% of the rated power and the upper limit being the rated power.

4) Fuel cell power constraint

$$
P_{fc}^{max}(t) = \min\left\{ P_{fc.N}, \frac{Q_{ht}(t) - Q_{htmin}}{\mu \bullet \Delta t} \bullet \eta_{fc} \right\}
\tag{37}
$$

where, $Pfc\ max(t)$ is the maximum output of the fuel cell at sampling time t; $P_{fc.N}$ is the rated output of the fuel cell; $Q_{ht}(t)$ is the storage capacity of the hydrogen tank at sampling time t; Q_{htmin} is the lower capacity limit of the hydrogen tank.

5) Hydrogen production constraint of electrolysis cells

$$
Q_{el}^{max}(t) = \min\left\{ Q_{el.N}, \frac{Q_{ht\,max} - Q_{ht}(t)}{\eta_{el} \bullet \rho \bullet \Delta t} \right\}
\tag{38}
$$

where, $Qmax\ el(t)$ is the maximum hydrogen production of the electrolyzer at sampling time t; $Q_{el.N}$ is the nominal hydrogen production of the electrolyzer; Q_{htmax} is the maximum capacity of the hydrogen storage tank.

6) Capacity constraints of hydrogen storage tanks

$$
Q_{htmin} \leq Q_{ht} \leq Q_{htmax}
\tag{39}
$$

where, $Q_{htmin} = 0.1Q_{htmax}$, and $Q_{htmax} = 0.9Q_{ht.N}$ ($Q_{ht.N}$ is the nominal storage capacity of the hydrogen tank).

4. Model Solving

The capacity configuration of a wind-hydrogen hybrid energy storage system is a multi-objective, multi-constrained, multi-variable non-linear optimization problem, and the system economy and reliability cannot be optimal at the same time. Given that the NSGA-II algorithm has the advantages of high operational efficiency, good distribution of the solution set and good convergence of the solution set, the NSGA-II multi-objective genetic optimization algorithm is used here to solve the capacity allocation scheme of the hybrid energy storage system, and the solution flow is shown in Figure 4.
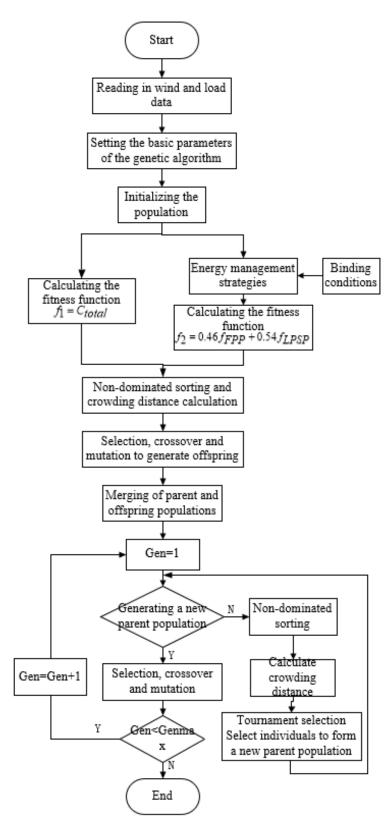
Figure 4. Flow of capacity optimization

5. Example Analysis

To verify the effectiveness of the proposed capacity optimization method, a typical daily load and wind velocity in a pastoral area of Inner Mongolia were selected as the system input data, with a sampling interval of 10 min and a wind turbine capacity of 60 kW. Typical daily wind speed and load curves are shown in Figure 5 and Figure 6.
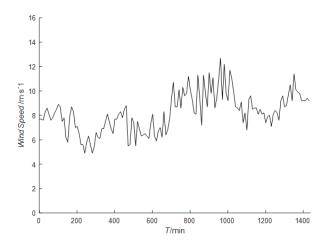
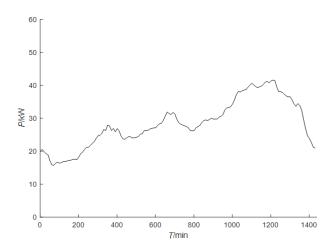**Figure 5.** Daily wind velocity data

Figure 6. Daily load data

The actual output power of wind turbine can be obtained from the wind speed data in Figure 5 and formula (1), as shown in Figure 7.
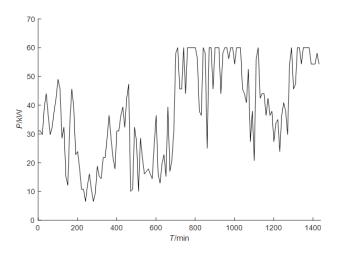

Figure 7. Output power of wind turbine

The power curve of the hybrid energy storage device is obtained from the difference between the wind turbine output and the load demand, as shown in Figure 8.
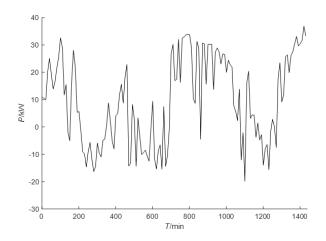
Figure 8. Energy storage units power

Before capacity optimization, the optimization interval of C_{EL}, C_{SC} are set to 0~40kW, and the optimization interval of C_{FC}, C_{HT} are 0~30kW and 0~1000Nm³ respectively, this is because when the wind turbine output is greater than the load demand, the power dissipated by the electrolytic tank and the battery does not exceed 40kW, and conversely when the wind power output is insufficient, the total regulated power of the fuel cell and the battery is less than 30kw. The initial SOC of the battery and hydrogen storage system is 50%.

The installation costs and related parameters of hydrogen storage and batteries are shown in Table 2.

Table 2. Energy storage parameters of wind hydrogen system

Equipment name	Unit investment cost(¥/kW)	Proportion of O&M cost(%)	Service life (yeras)	Efficiency (%)
Electrolysis cell	$1.4×10^4$	5	10	75
Battery	$1.2×10^3$	1	4	85/95
Fuel cell	$1.4×10^4$	5	10	60
Hydrogen storage tank	$3.3×10^3$	1	20	95

The NSGA-II sets the number of populations to 100, the maximum number of iterations to 200, the crossover probability to 0.8 and the mutation probability to 0.2. Figure 9 shows the Pareto optimal solution set after the algorithm has been solved, and the analysis shows that the capacity of the energy storage device is linearly related to the reliability of the power supply. On the contrary, when the capacity of energy storage is low, the economy can be guaranteed but the reliability of the supply cannot be taken into account. The economic cost of the system, the power fluctuation rate and the reliability of the supply are all in conflict with each other and cannot be solved optimally at the same time.
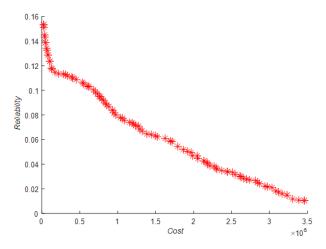

Figure 9. Pareto solution set

In order to find the optimal solution that satisfies both the lowest economic cost and the highest supply reliability, a solution from the Pareto solution set frontier needs to be found as a configuration solution of a hybrid energy

60

storage device of wind-hydrogen systems. Table 3 to Table 4 show the obtained set of Pareto optimal solution sets with the corresponding energy storage capacity.

Table 3. A set of Pareto optimal solutions

Options	Economic cost×10^6/¥	Reliability
1	3.4463	0.0104
2	0.0446	0.1396
3	0.9659	0.0813
4	1.7744	0.0560
5	0.6527	0.1011
6	1.9316	0.0494
7	2.0468	0.0452
8	1.5845	0.0607
9	0.1007	0.1270
10	2.5563	0.0320

Table 4. Capacity configuration options

Options	Electrolysis cell /kW	Battery/kWh	Fuel cell/kW	Hydrogen storage tank /Nm³
1	35.8215	39.3740	16.7600	492.4003
2	0.1041	5.3393	0.0914	0.4587
3	25.9401	33.3283	0.0914	0.4587
4	28.3054	39.3740	9.8782	122.6094
5	15.5287	33.7735	0.0914	0.4587
6	26.8001	37.9503	16.7585	122.6094
7	30.1488	39.1573	16.7600	124.7478
8	28.8913	39.9808	9.8782	59.3710
9	0.5291	13.9939	0.0914	0.4587
10	27.4335	39.3740	16.7600	302.0766

Considering the economic cost and the reliability of the power supply, the relative optimal solution is chosen according to the principle of compromise. The total cost of option 6 is less than $2×10^6$ ¥ and the reliability index reaches 0.0494, i.e., the load outage rate and power fluctuation rate are less than 10% at this time. This option ensures safe and reliable power supply on the premise of minimizing system cost, therefore option 6 is chosen as the final optimization option.
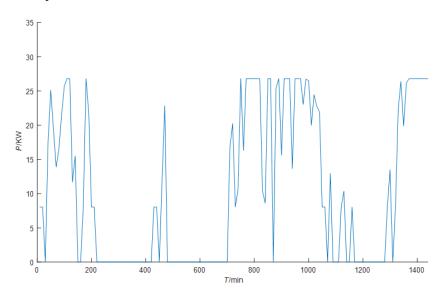

Figure 10. Power of electrolytic cell

Figure 10 and Figure 11 show the input power of the electrolyzer and the hybrid energy storage charge state under this scheme. It is clear that when the wind power output is less than the load demand, the energy management strategy of giving priority to the discharge of the battery over the fuel cell is satisfied; As a flexible energy storage unit, the battery is charged and discharged more frequently than hydrogen storage and can assist the electrolyzer to produce hydrogen efficiently; the energy management strategy is developed to keep the electrolyzer in the

optimal operating range(minimum operating power of the electrolytic cell is 8kw and maximum operating power is 26kw), avoiding intermittent operation and frequent start-ups and stoppages of the electrolyzer, thus improving its hydrogen production efficiency and service life to a certain extent and ensuring safe operation and stable hydrogen production.
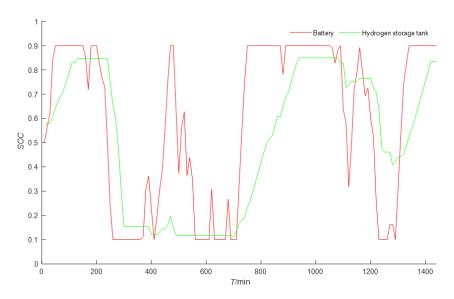

Figure 11. State of charge of hybrid energy storage

6. Conclusions

Taking into account the hydrogen production features of the electrolyzer, this paper develops an energy management strategy that applies to six operating conditions, and a method for optimizing the energy storage capacity with good economy, high hydrogen production efficiency and good reliability is proposed. The following conclusions are obtained by analyzing the results of arithmetic examples:

(1) In the results of solving the proposed optimization model, a set of low-cost and reliable capacity configuration solutions were found (electrolyzer 26.8001/kW, battery 37.9503/kWh, fuel cell 16.7585/kW, hydrogen storage tank 122.6094/Nm^3, economic cost 1.9316×106/¥, reliability indicator 0.0494).

(2) The developed energy management strategy can maximize the operation of the electrolyzer in the optimal working range (30%~100% of rated power), ensure efficient hydrogen production, avoid intermittent operation and frequent start/stop of the electrolyzer, and improve the service life of the equipment.

(3) The proposed energy management strategy and capacity optimization method can provide reference for the actual capacity configuration study of wind-hydrogen storage systems. However, the capacity optimization model is constructed with economic indicators that do not take into account the revenue from hydrogen sales. At this stage, the investment cost and conversion efficiency of fuel cells are still low, so it may be more economical to sell hydrogen regularly to the nearest hydrogen market for profit, in addition to supplying electricity.

Data Availability

The data used to support the findings of this study are available from the corresponding author upon request.

Conflicts of interest

The authors declare that they have no conflicts of interest.

Funding

References

[1] Z. Y. Yan and X. W. Kong, "Research on non-grid-connected wind power water-electrolytic hydrogen production system and its applications," *Strateg. Study CAE*, vol. 17, no. 3, pp. 30-34, 2015.

[2] C. Y. Nie, X. J. Shen, H. Lv, and W. Wang, "Capacity Configuration and control strategy of hydrogen super hybrid energy storage in grid connected wind farm," *Smart Power*, vol. 48, no. 9, pp. 1-8, 2020. https://doi.org/10.3969/j.issn.1673-7598.2020.09.002.

[3] K. X. Liang and H. Lin, "Wind-hydrogen system's hybrid energy storage capacity optimization considering equipment features," *Modern Electron. Technique*, vol. 44, no. 21, pp. 180-186, 2021. https://doi.org/10.16652/j.issn.1004-373x.2021.21.037.

[4] J. C. Zhao, J. Chen, and X. J. Ma, "Energy storage capacity optimization for wind power /hydrogen system considering dispatching program and economy," *Electr. Meas. & Instrum.*, vol. 55, no. 24, pp. 94-99, 2018.

[5] G. W. Cai, L. G. Kong, A. X. Xu, and Z. X. Li, "Evaluation of wind/Hydrogen/Fuel cell grid-connected system power smoothing based on improved chemical reaction optimization algorithm," *T. China Electrotechnical Soc.*, vol. 20, pp. 251-260, 2017. https://doi.org/10.19595/j.cnki.1000-6753.tces.161037.

[6] R. G. Ma, J. Chen, J. C. Zhao, H. W. Zhang, and M. Sun, "Multi-objective optimization for capacity of non-grid-connected wind/hydrogen hybrid power system," *Acta Energiae Solaris Sinica*, vol. 40, no. 2, pp. 422-429, 2019.

[7] W. Zhang, A. Maleki, F. Pourfayaz, and M. S. Shadloo, "An artificial intelligence approach to optimization of an off-grid hybrid wind/hydrogen system," *Int. J. Hydrogen Energy*, vol. 46, no. 24, pp. 12725-12738, 2021. https://doi.org/10.1016/j.ijhydene.2021.01.167.

[8] W. Zhang, A. Maleki, M. A. Rosen, and J. Liu, "Sizing a stand-alone solar-wind-hydrogen energy system using weather forecasting and a hybrid search optimization algorithm," *Energ. Convers. Manage.*, vol. 180, pp. 609-621, 2019. https://doi.org/10.1016/j.enconman.2018.08.102.

[9] S. Basu, A. John, and A. Kumar, "Design and feasibility analysis of hydrogen based hybrid energy system: A case study," *Int. J. Hydrogen Energy*, vol. 46, no. 70, pp. 34574-34586, 2021. https://doi.org/10.1016/j.ijhydene.2021.08.036.

[10] G. W. Cai, L. G. Kong, Y. Xue, and B. Z. Sun, "Overview of research on wind power coupled with hydrogen production technology," *Autom. Electric Pow. Systems*, vol. 38, no. 21, pp. 127-135, 2014. https://doi.org/10.7500/AEPS20131231004.

[11] J. Li, G. Li, D. Liang, and S. Ma, "Review and prospect of hydrogen production technology from renewable energy under targets of carbon peak and carbon neutrality," *Distrib. Energy*, vol. 6, no. 5, pp. 1-9, 2021. https://doi.org/10.16513/j.2096-2185.de.2106528.

[12] A. Villagra and P. Millet, "An analysis of PEM water electrolysis cells operating at elevated current densities," *Int. J. Hydrogen Energy*, vol. 44, no. 20, pp. 9708-9717, 2019. https://doi.org/10.1016/j.ijhydene.2018.11.179.

[13] Z. Hong, Z. Wei, and X. Han, "Optimization scheduling control strategy of wind-hydrogen system considering hydrogen production efficiency," *J. Energy Storage*, vol. 47, Article ID: 103609, 2022. https://doi.org/10.1016/j.est.2021.103609.

[14] "EU Harmonised Polarisation Curve Test Method for Low Temperature Water Electrolysis," JRC104045, 2018, Luxembourg: Publications Office of the European Union.

[15] Y. Fang, J. Chen, and X. Z. Tian, "Capacity economical optimization of non-grid-connected wind/hydrogen hybrid micro power grid," *Comput. Simulat.*, vol. 37, no. 2, pp. 110-114, 2020.

[16] Z. H. Deng and Y. W. Jiang, "Optimal sizing of a wind-hydrogen system under consideration of the efficiency features of electrolysers," *Renew. Energy Resour.*, vol. 38, no. 2, pp. 259-266, 2020. https://doi.org/10.13941/j.cnki.21-1469/tk.2020.02.018.

[17] W. Dong, Y. Li, and J. Xiang, "Optimal sizing of a stand-alone hybrid power system based on battery/hydrogen with an improved ant colony optimization," *Energies*, vol. 9, no. 10, Article ID: 785, 2016. https://doi.org/10.3390/en9100785.

[18] A. Maleki, "Design and optimization of autonomous solar-wind-reverse osmosis desalination systems coupling battery and hydrogen energy storage by an improved bee algorithm," *Desalin.*, vol. 435, pp. 221-234, 2018. https://doi.org/10.1016/j.desal.2017.05.034.

[19] A. Emrani, A. Berrada, A. Arechkik, and M. Bakhouya, "Improved techno-economic optimization of an off-grid hybrid solar/wind/gravity energy storage system based on performance indicators," *J. Energy Storage*, vol. 49, Article ID: 104163, 2022. https://doi.org/10.1016/j.est.2022.104163.

[20] A. Mahesh and K. S. Sandhu, "A genetic algorithm based improved optimal sizing strategy for solar-wind-battery hybrid system using energy filter algorithm," *Front. Energy*, vol. 14, no. 1, pp. 139-151, 2020. https://doi.org/10.1016/j.est.2022.104163.